Available online at www.sciencedirect.com
SCIENCE DIRECT
Journal of Power Sources 157 (2006) 64–77
JOURNAL OF POWER SOURCES
www.elsevier.com/locate/jpowsour

Preferential CO oxidation on Ru/Al_2O_3 catalyst: An investigation by considering the simultaneously involved methanation

Guangwen Xu [a,b], Zhan-Guo Zhang [a,*]

[a] *National Institute of Advanced Industrial Science and Technology (AIST), 2-17 Tuskisamu-Higashi, Toyohira-ku, Sapporo 062-8517, Japan*
[b] *Institute of Processing Engineering, The Chinese Academy of Sciences, P.O. Box 353, Beijing 100080, China*

Received 5 July 2005; accepted 10 July 2005
Available online 24 August 2005

Abstract

The CO removal with preferential CO oxidation (PROX) over an industrial 0.5% Ru/Al_2O_3 catalyst from simulated reformates was examined and evaluated through considering its simultaneously involved oxidation and methanation reactions. It was found that the CO removal was fully due to the preferential oxidation of CO until 383 K. Over this temperature, the simultaneous CO methanation was started to make a contribution, which compensated for the decrease in the removal due to the decreased selectivity of PROX at higher temperatures. This consequently kept the effluent CO content as well as the overall selectivity estimated as the ratio of the removed CO amount over the sum of the consumed O_2 and formed CH_4 amounts from apparently increasing with raising reaction temperature from 383 to 443 K when the CO_2 methanation was yet not fully started. At these temperatures the tested catalyst enabled the initial CO content of up to 1.0 vol.% to be removed to several tens of ppm at an overall selectivity of about 0.4 from simulated reformates containing 70 vol.% H_2, 30 vol.% CO_2 and with steam of up to 0.45 (volume) of dry gas. Varying space velocity in less than 9000 h^{-1} did not much change the stated overall selectivity. From the viewpoint of CO removal the article thus concluded that the methanation activity of the tested Ru/Al_2O_3 greatly extended its working temperatures for PROX, demonstrating actually a feasible way to formulate PROX catalysts that enable broad windows of suitable working temperatures.

Keywords: Selective CO oxidation (PROX); Methanation; Polymer electrolyte fuel cell (PEFC); Hydrogen purification; Ru catalyst

1. Introduction

Running the polymer electrolyte fuel cell (PEFC) on reformates of various hydrocarbon fuels requires a gas cleanup facility to remove CO in the hydrogen-rich reformate to several tens of ppm (i.e. 10s ppm), preferably to less than 10 ppm [1–3]. In theory, there are several physio-chemical methods, which can be employed for the facility to remove CO or to separate H_2 from the other gas components (e.g., CO_2, CO, etc.). These include the pressure swing adsorption (PSA [4]), Pd-membrane diffusion [5–7], CO methanation (both non-competitive [8] and selective [6–8]), electrolytic CO oxidation [9] and preferential CO oxidation [4–7,10]. As for the use in PEFC systems, the suitable and presently technique-possible method may be only the preferential CO oxidation (PROX) [3,5,11], resulting in the extensive studies in last decade on it in both catalyst development [5,12] and reactor design [7,13,14]. The early report about PROX can date back to the 1960s [15]. Then, Oh and Sinkevitch [16] evaluated the catalytic suitability of a variety of alumina-supported metallic materials (Pt, Pd, Rh, Ru, Co/Cu, Ni/Co/Fe, Ag, Cr, Fe and Mn). Succeeding that work, many studies were carried out to formulate high-efficient and high-selective catalysts for PROX with different noble (including Au and Ag) and base metals [5,12]. In practices, however, the common catalyst formulations are still based on Pt-group elements, for their high reliability in applying to various other catalytic reactions [4–7,12–14]. The favorite use of the Pt-family catalysts for PROX is also due to the reaction temperatures of these cata-

* Corresponding author. Tel.: +81 29 861 8091; fax: +81 29 861 8209.
E-mail address: z.zhang@aist.go.jp (Z.-G. Zhang).

0378-7753/$ – see front matter © 2005 Elsevier B.V. All rights reserved.
doi:10.1016/j.jpowsour.2005.07.028

lysts for PROX, which are generally from 373 to 473 K and just fit in with the working temperatures of the upstream WGS reactor (∼473 K) and downstream PEFC stack (∼253 K).

Of the five elements in Pt-group metals, the catalysts formulated with Pt (particularly Pt/Al_2O_3) have been most extensively tested [4,16–20]. The CO conversion over the catalysts, however, is highly sensitive to reaction temperature so that there is usually a narrow range (e.g., <20 K) of suitable temperatures for operation [14,17–19]. Changing formulations of the catalysts may widen their working temperature windows, but the available examinations are limited to laboratory scales [21,22]. On the other hand, the Ru-based catalysts, especially Ru/Al_2O_3, are also commonly available, while they have been shown to be more efficient for oxidizing CO than the other catalysts based on Pt, Pd, Rh and Co (under normal pressure conditions [23]). In fact, Ru/Al_2O_3 was already demonstrated to enable the better CO removal performance than Pt/Al_2O_3 in a few works [16,24–27]. This may be why the Ru-based catalysts, including Pt-Ru alloy catalysts, are widely used in the presently existing practical PROX reactors and processes [13,14,25,28,29].

However, the public information about the PROX performance of Ru catalysts is very limit, compared to the prolific reports about Pt catalysts. An early study of Brown and Green [15] on an industrial 0.5% Ru/Al_2O_3 showed that the required O_2-to-CO atomic ratio (O/CO ratio) increases with increasing the initial CO content and it must be higher than 3.5 (v/v) for oxidizing 0.5 vol.% CO down to 10 ppm in a hydrogenous gas containing about 60 vol.% H_2, 20 vol.% CO_2 and 20 vol.% N_2. The suitable temperatures were said to be 395–435 K. With a N_2-base gas containing 0.85 vol.% H_2, 900 ppm CO and 800 ppm O_2, Oh and Sinkevitch [16] realized CO removals of up to 100% at temperatures between 375 and 575 K on a commercial 0.5% Ru/Al_2O_3. Compared to the narrower temperature range of Brown and Green [15], the wider working temperature window in the latter case would be a result of its lower H_2 content in the treated gas. The recently available data about PROX over Ru-based catalysts are limited to a few literature reports [13,14,24–33]. Most of the works dealt with the formulation and characterization of the catalysts prepared for their own specified PROX reactors or fuel processors [13,14,25–29] or just for laboratory tests [30–33]. Hence, the documented results are less systematic and less general, even divergent. While Abdo et al. [30] reported viable PROX-suitable temperatures from 343 to 433 K for their impregnated Ru (0.5–3.0 wt.%) on a porous alumina, Utaka et al. [33] identified a temperature window between 513 and 573 K over their own 2% Ru/Al_2O_3 formulation. Over a 5% Ru/γ-Al_2O_3 reduced in pure H_2 at 423 K, Han et al. [26,27] preferred the working temperatures below 423 K so that the simultaneous CO and CO_2 methanations can be completely avoided. Different O/CO ratios varying from 3.0 (v/v) [14,32] to 6.0 (v/v) [28–30] were also demonstrated to be necessary for oxidizing CO down to lower than 100 ppm in simulated reformates containing 0.5–1.0 vol.% CO. Therefore, we are indeed lacking systematic characterization of the PROX performance of Ru catalysts, especially of the commercially available Ru catalysts that would be most possibly used for practical PROX reactors.

Moreover, the Ru catalysts are also highly active to CO and CO_2 methanations [34–36]. The aforementioned literatures, however, disregarded this or simply treated it as a minor point. The CO methanation may positively affect the CO abatement with PROX over Ru catalysts [25,37,38], although it is generally treated as an undesired side reaction [24–27,33]. Thus, without considering the simultaneous CH_4 formation with PROX one may never fully understand the causes for the better CO removal performance of Ru catalysts. Recently, Han et al. [26,27] revealed that the methanations of CO and CO_2 with PROX on a 5% Ru/Al_2O_3 in methanol reformate are negligible at temperatures below 423 K, causing their insistence on operating the PROX over the catalyst at temperatures not over 423 K. However, it is questionable if the methanation of CO is truly deadly undesirable for PROX.

The present article tested the PROX over an industrial 0.5% Ru/Al_2O_3 catalyst, under an intention of examining and further evaluating its CO removal performance with consideration of the simultaneously involved oxidation and methanation reactions. Succeeding experimental measurements of both the CO removal and CH_4 formation with PROX over the catalyst, the further evaluation of the acquired CO removal in terms of an overall selectivity and its accompanied H_2 loss clarified how the methanation activity of the catalyst affected the CO removal efficiency and effectiveness (i.e. selectivity). It was shown that the simultaneously involved CO methanation much broadened the catalyst's suitable temperature window for PROX in the view of removing CO, whereas its induced additional H_2 loss was not significant at the suitable temperatures that assured as well the preferential methanation of CO. Consequently, the article concluded that a highly active catalyst for PROX is better to have a high activity for methanation in order to selectively removing CO in a wide temperature window.

2. Experimental

2.1. Catalyst and reactant gases

The adopted 0.5% Ru/Al_2O_3 catalyst was characterized in Table 1, which was from N.E. Chemcat Corporation and had a cylindrical-pellet shape in size of Ø 3.2 mm × 3.5 mm. Its average bulk density and BET surface area were 950 kg m^{-3} and 92.9 m^2 g^{-1}, respectively. The catalyst contained mesopores in sizes of 3.2–38.5 nm, but most pores had diameters around 6.8 nm (by N_2 adsorption/desorption at 77 K in BELSORP28, Bel Japan). The Ru dispersion of the original catalyst determined from CO adsorption was about 60%.

All tested reformates were based on a H_2-to-CO_2 volumetric ratio (dry-base) of about 70/30 (fluctuated in ±1.0) and their CO contents varied from 0.1 to 1.0 vol.%. Pure O_2 was additionally added as the oxidant according to the desired

Table 1
Characterization of the adopted catalyst and reactors

Catalyst (Commercially available from *N.E. Chemcat Corp.*)

Composition	0.5%Ru/Al_2O_3	*Shape*	Cylindric pellet
Size	ϕ3.2×3.5 mm	*Bulk density*	950 kg/m^3
Bet surface	92.9 m^2/g	*Meso-pore sizes*	3.2-38.5nm

Ru dispersion (determined from CO adsorption): about 60%

Stainless-steel-made reactor (Fixed bed, as is illustrated below)

Heating: Current-controlled tape heaters
Gases: From gas cylinders
Flow control: Mass flow meters
Steam: Water pump + Evaporator
Gas analysis: Micro TCD GC
Temp. measurement: Thermocouple in catalyst

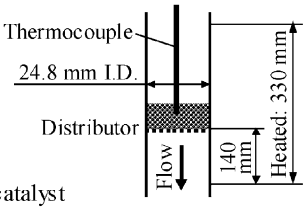

Quartz reactor (Fixed bed, 23.0 mm in I.D.)

Heating: Gold-coated furnace (300 mm long)
Temp. measurement: Thermocouple in a thermo-well (see illustration)
All others: Similar to those for the metallic reactor

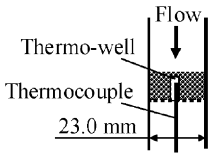

O/CO ratio. There were not other alien gases, such as CH_4, N_2 and CH_3OH added to the initial dry feed. In the case of exploring the influences of CO_2 and H_2 fractions (see Fig. 7), the volumetric flow rate of CO_2 or H_2 was varied with a corresponding balanced change in the H_2 or CO_2 flow rate so that the total flux of H_2 and CO_2 remained as a constant. All the quoted gas components were from their respective cylinders under controls of mass-flow meters. They then mixed together and finally entered one of the reactors specified in Section 2.2.

Steam's influence on the performance of the catalyst for removing CO and producing CH_4 was investigated by adding steam of up to 45% (volumetric) of dry gas into the aforementioned simulated reformates. This highest steam ratio was suggested to be typical for the gas streams after WGS because the steam-to-CH_4 molar ratio in the upstream reformer ranged usually from 3.0 to 5.0 (v/v) (high-C hydrocarbons requiring lower steam-to-C ratios due to their lower reforming temperatures). Steam was generated in a steel-ball packed water evaporator, a stainless-steel pipe of 30 mm i.d., and was carried with the reactant H_2. The other gas components, i.e. CO_2, CO and O_2, were added to the H_2–steam stream at the exit of the evaporator so as to avoid the possible reverse WGS (RWGS) reaction inside the evaporator. While the steam generator ran generally at 473 K or so, the pipes between the steam generator and PROX reactor were warmed (only when steam was fed) up to 373 K to prevent steam condensation. The steam amount was controlled through measuring the water amount fed to the evaporator with a high-pressure micro liquid pump (L-7110, Hitachi).

2.2. Apparatus and methods

Noting that all practical PROX operations are in metallic reactors, we performed most of the tests in a stainless-steel-made fixed-bed reactor of 24.8 mm i.d. As illustrated in Table 1, the reactor was electrically heated with wire-type heaters wrapping about the reactor, and a sintered-plate distributor supported the catalyst. In the catalyst bed a sheathed K-type thermocouple measured the reaction temperature. A PID controller controlled the temperature and also adjusted the current passing through the heater wires. This thus allowed the control of the temperature rising speed during heating the reactor (see Fig. 1a).

A blank test without catalyst load in the reactor demonstrated that the metals of the reactor had not catalytic effect on the investigated reactions, i.e. reactions (1)–(5) shown in Section 2.3, until 450 K. At higher temperatures (up to 520 K), slight CH_4 formation and CO removal were identified but the removed CO was less than 10% of its feed and the formed CH_4 was not over 500 ppm. Hence, it was convinced that the reactor materials little affected the present examinations since, as will be shown in Section 3, the tests in this article were basically at temperatures below 450 K. This little effect of reactor's metals was also verified through a measurement within a quartz reactor (Fig. 2). The employed quartz reactor had an i.d. of 23.0 mm (Table 1) and was heated in a gold-coated furnace. A thermocouple within a thermo-well that extended into the catalyst bed from the bed distributor, a ceramic plate, measured the reaction temperature. A power supply facility (CHINO SU12) coupling the furnace

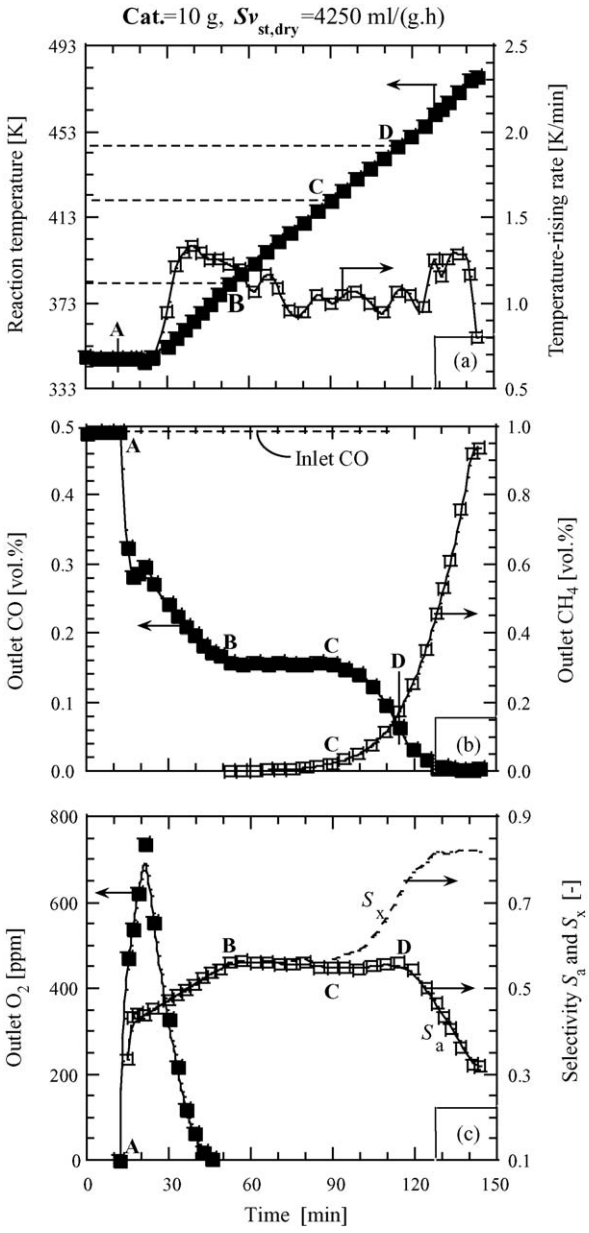

Fig. 1. (a–c) Screening the suitable reaction temperatures for CO removal over the tested catalyst. Feed gas (vol.%): 70.1 H_2 + 29.1 CO + 0.50 CO + 0.30 O_2. (a) A well-controlled temperature rise in the reactor. Affected by reaction heat, the rising rate was slightly higher in response to the rapid increase in oxidation around point B and in methanation by the end of the test.

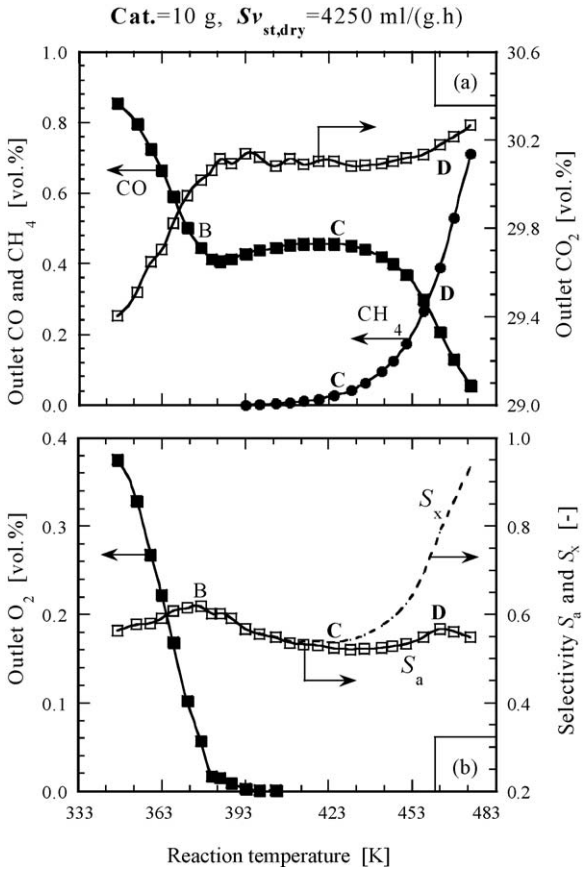

Fig. 2. (a and b) Further demonstration of the suitable temperatures for CO removal over the tested catalyst in a quartz reactor. Feed gas (vol.%): 69.4 H_2 + 29.1 CO + 1.00 CO + 0.51 O_2. Temperature control was similar to Fig. 1.

controlled the reactor temperature as well as the temperature-rising rate.

For both the metallic and quartz reactors, the thermocouple was positioned at the central level of the catalyst bed. Ten grams non-smashed catalyst was packed in the reactor, which created a catalyst bed of about 20 mm high. The molar compositions of reactant and reacted gases were measured using a two-channel micro TCD gas chromatograph (Micro GC, P200H). Monitoring the inlet gas composition with the GC data to adjust the O/CO ratio was possible during the reaction. A gas suction flow of about 50 ml min^{-1} provided the sample for the TCD analysis. Before entering the GC, the sample gas was drained and further dried in a $CaCl_4$ column. The GC P200H allowed CO and CH_4 concentrations lower than 10 ppm to be detected.

The test was started with reducing the catalyst in an argon–hydrogen stream (10 vol.% H_2) of 60 ml min^{-1} via a temperature program that first increased the temperature of the catalyst bed to 673 K at rates less than 100 K h^{-1} and then kept it there for 30 min. Decreasing the bed temperature from 673 K to experimental ones was realized by naturally cooling the reactor in the Ar–H_2 stream. The flow switch from the Ar–H_2 to a simulated reformate (with O_2 as well) then started the reactions. When steam feed was required, the gas switch was made between the Ar–H_2 and H_2–steam streams, and subsequently the other gas components were added.

2.3. Parameter definitions

The article defined the space velocity as the ratio of either dry- or wet-base gas volume under the conditions of 1.0 atm and 273 K over grams of catalyst, which is denoted herein as $S_{v(st,dry)}$ or $S_{v(st,wet)}$, respectively.

The possible reactions in a PROX reactor are as follows:

$$\text{CO oxidation}: \quad CO + \tfrac{1}{2}O_2 \rightarrow CO_2, \tag{1}$$

$$H_2 \text{ oxidation}: \quad H_2 + \tfrac{1}{2}O_2 \rightarrow H_2O, \tag{2}$$

$$\text{CO methanation}: \quad CO + 3H_2 \rightarrow CH_4 + H_2O, \tag{3}$$

$$CO_2 \text{ methanation}: \quad CO_2 + 4H_2 \rightarrow CH_4 + 2H_2O, \tag{4}$$

and

$$\text{WGS and RWGS}: \quad CO + H_2O \leftrightarrow H_2 + CO_2. \tag{5}$$

Usually, the WGS toward the right side of reaction (5) is weak when the CO content in the feed is less than 1.0 vol.%. The undesired RWGS to the left side of reaction (5) may surely occur at high temperatures (>480 K), but we can treat it as an internal reaction that reduces the CO removal by increasing the CO amount in the reactor. Overall, the system can thus be treated as a CO cleanup "box", which removes CO via consuming O_2 in reaction (1) and releasing CH_4 through reaction (3). Reactions (2) and (4), on the other hand, occur to cause wasteful O_2 and H_2 consumptions, respectively. These definitely degrade the efficiency of CO removal, thus rending the use of the conventionally defined "oxidation" selectivity, i.e.

$$S_x = \frac{\text{removed CO}}{2 \times \text{consumed O}_2} = \frac{[CO]_{inlet} - [CO]_{outlet}}{2([O_2]_{inlet} - [O_2]_{outlet})}, \tag{6}$$

apparently unreasonable because this seriously overestimates the performance of the catalyst when reaction (3) or (4) occurs to a considerable degree to make its H_2 consumption not negligible. Thus, the "overall" selectivity S_a considering not only O_2 consumption but also CH_4 formation was newly introduced, as

$$S_a = \frac{\text{removed CO}}{2 \times \text{consumed O}_2 + \text{formed CH}_4} = \frac{[CO]_{inlet} - [CO]_{outlet}}{2([O_2]_{inlet} - [O_2]_{outlet}) + [CH_4]_{outlet}}, \tag{7}$$

to evaluate the performance of the tested catalyst for removing CO. In Eq. (7), the latter formulation neglected the change of gas volume through the reactor, which should be reasonable except that the initial O_2 supply or the concentration of formed CH_4 was extremely high.

For a practical CO-cleanup setup, to know its hydrogen loss or consumption is critical. The above-defined selectivities, especially S_a, somehow measure the loss but the losing amount is not directly visible. Thus, an "absolute" H_2 loss H_{sa} was also introduced into the article to evaluate the totally reacted H_2 through reactions (2)–(4). The RWGS consumes H_2 as well, but the formed CO might increase the consumption of O_2 through reaction (1), which in turn compensatively reduce the H_2 consumption via reaction (2). Reactions (3) and (4) have different H_2-consumptions in forming 1 mol CH_4. The CO methanation via reaction (3), however, is dominant or nearly fully prior to that of CO_2 via reaction (4) under the adaptive conditions for PROX, as will be shown in our results throughout Section 3. Consequently, we have

$$\begin{aligned} H_{sa} &= (2 \times \text{consumed O}_2 - \text{oxidized CO}) + 3 \times \text{formed CH}_4 \\ &= 2 \times \text{consumed O}_2 - \text{reduced CO} + 4 \times \text{formed CH}_4. \end{aligned} \tag{8}$$

In Eq. (8), we suggested that the "oxidized CO" via reaction (1) is equal to the difference between the totally "reduced CO" and "formed CH_4". This suggestion is again based on the assumption that CO methanation is fully prior to that of CO_2. On the other hand, the second formula of Eq. (8) shows that the estimated absolute H_2 loss H_{sa} is equivalent to a H_2 computation by assuming that all removed CO is due to CO oxidation through reaction (1) and all formed CH_4 is from CO_2 methanation via reaction (4). In this sense, we can see that Eq. (8) predicts actually the real H_2 loss. That is, when there is x mol CH_4 produced from CO methanation, both the formed CH_4 from CO_2 methanation and the oxidized CO in reaction (1) surely decrease x mol so that the net change in the reacted H_2 amount becomes $(x + 3x) - 4x = 0$, where the released x mol O (or $1/2O_2$) from decreased CO oxidation is supposed to oxidize x mol H_2 according to reaction (2), and $3x$ and $4x$ refer to the moles of reacted H_2 in CO and CO_2 methanations, i.e. in reactions (3) and (4), respectively.

Corresponding to S_x, we can also have the conventional H_2 loss

$$H_{sx} = 2 \times \text{consumed O}_2 - \text{reduced CO} \tag{9}$$

which considers only the reacted H_2 with overfed O_2. Thus, the difference between H_{sx} and H_{sa} measures how the methanation contributes to the total H_2 loss.

3. Performance examination

3.1. Adaptive operating parameters

3.1.1. Temperature window

Fig. 1 shows the result of a test under programmed temperatures (a) for a reactant gas containing 0.5 vol.% CO and 0.3 vol.% O_2 (O/CO = 1.2). The dry-base space velocity was 4250 ml g^{-1} h^{-1}. Without O_2 feed, the CO concentration at the outlet (left Y of Fig. 1b) quickly reached its inlet value in about 15 min at about 345 K (point A). This thus excluded the possible contribution of CO adsorption on the catalyst to the subsequent CO removal under the conditions with O_2 supply. Feeding O_2 at point A caused an immediate decrease in the outlet CO content, showing that the examined catalyst has readily some high activity to oxidize CO at temperatures below 345 K. After a quarter of an hour to stabilize the O_2 supply, the reactor was then heated to raise the reaction temperature at a rate of 1.0 K min^{-1} or so (right Y in Fig. 1a). In response, the outlet CO content exhibited three distinctive variation regions, say, the quick decreases before B (~383 K)

and after C (~423 K) and the remaining in a constant in-between. The lowest outlet CO content reached 10s ppm at temperatures higher than 463 K (>130 min), revealing actually a weak RWGS for the test. The fact behind the result may be that the RWGS truly occurred but the formed CO was subsequently methanated (will be further explained), implicating that the methanation activity of the tested Ru catalyst positively affected its CO removal performance. Without this activity, most other PROX catalysts, such as Pt/Al_2O_3, suffer usually an obvious performance degradation from RWGS at high temperatures [24–26].

The accompanying CH_4 formation is shown in right *Y* of Fig. 1b. After it became detectable at point B, the formed CH_4 got gradually more with raising the temperature, but until point C the formed CH_4 amount was slight so that the outlet CH_4 fraction was not over 250 ppm at C. Then, the outlet CH_4 fraction rapidly increased with temperature and reached about 0.4 vol.% when the outlet CO content approached 10s ppm at about 130 min. There was thus an extract correspondence between the increase in CH_4 formation (hundreds of ppm to 0.4 vol.%) and decrease in outlet CO content (0.2 vol.% to 10s ppm) from point C, demonstrating essentially the CO methanation in prior to CO_2 methanation. This, while verifying a few literatures [7,9], indicates that the promoted CO removal after C must be due to CO methanation.

The O_2 fraction in the outlet gas stream was shown in Fig. 1c via left *Y*. Shortly after O_2 feed, the outlet O_2 concentration first increased to indicate a time delay in responding to feeding. Then, it decreased with increasing temperature until the fed O_2 was completely consumed at about 370 K. The calculated selectivities S_x from Eq. (6) and S_a from Eq. (7) were plotted in right *Y* of Fig. 1c. Both S_a and S_x are identical till point C, just aligning with the slight CH_4 formation at these low temperatures. The selectivities first increased with temperature and subsequently stopped at a constant of about 0.55 between B and C. Raising temperature then caused S_x to further ascend but kept S_a until point D (445 K). After D, S_a rapidly decreased, whereas S_x gradually approached its highest possible value of 0.83 for the tested O/CO ratio of 1.2 (v/v).

The detailed understanding of the preceding variations in the outlet CO concentration and selectivities S_a and S_x with temperature will be presented in Section 4.1.1. On the basis of the data here we can judge that the suitable operating temperatures for PROX on the tested catalyst are preferably from 383 (point B) to 423 K (point C). The upside temperature (423 K) just consists with the statement of Han et al. [27], indicative essentially of the highest temperature allowing PROX without detectable CH_4 formation. Rather higher temperatures are beneficial to CO removal. Although this occurs with more CH_4 formation, the values of S_a indicate that the CO methanation is dominant until 445 K at point D (see more explanation in Section 4.1.1). Thus, if we further adopt this preferential CO methanation as a viable way to remove CO, the operating temperatures of the catalyst for CO abatement can be extended to 445 K. Furthermore, while S_x gradually increased from C, S_a was nearly a constant between B and D, indicating that the use of S_a, instead of S_x, is more reasonable for characterizing the CO removal performance of the Ru catalyst. Without considering the formed CH_4 in PROX, the conventionally defined selectivity S_x clearly overestimated the selectivity to CO oxidation in the region where CO methanation occurred to a certain extent (e.g., after C).

Fig. 2 further verifies the above temperature screening result through a similar test in the quartz reactor for a gas containing 1.0 vol.% CO at O/CO = 1.0 (v/v). The plots are against reaction temperature. Exactly as shown in Fig. 1b, the outlet CO content (left *Y* in Fig. 2a) had three variation regions demarcated at points B (~373 K) and C (~423 K), and the accompanying CH_4 formation (left *Y* in Fig. 2a) after point C was greatly enhanced by raising temperature. Measuring the CO_2 concentration in the effluent gas (right *Y* in Fig. 2a) clarified that the quick removal of CO before B and after C is due to CO oxidation and CO methanation, respectively. That is, while oxidizing CO to CO_2 evidently increased the outlet CO_2 content until B, the decreased dry gas volume with methanation only slightly elevated it after C. Without much CH_4 formation, both S_a and S_x (right *Y* in Fig. 2b) were coincident until C. The supplied O_2 was used up around B (left *Y* in Fig. 2b), but the outlet CO content slightly increased from B to C to lead to a corresponding decrease in S_a and S_x (see explanation in Section 4.1.1). The overall selectivity S_a, however, did not obviously decrease until point D (~463 K) or even after D, revealing the similar suitable temperatures of the catalyst for removing CO, which are from 373 to 463 K or preferably from 373 to 423 K.

3.2. O/CO ratio and space velocity

Fig. 3 shows the variations of outlet gas composition (CO, CH_4, CO_2 and H_2) with O/CO ratio at two typical suitable reaction temperatures (394 and 420 K). The feed gas had an initial CO concentration of 1.0 vol.%, and the space velocity was the same as that in Figs. 1 and 2 (4250 ml g^{-1} h^{-1}). The CO content (left *Y*) at the outlet decreased with raising the O/CO ratio. Removing the inlet CO to 10s ppm was realized at O/CO of about 2.3 (v/v) under both the temperatures, and for a given O/CO in 1.0–2.5 (v/v) the outlet CO content had not large difference between the tested temperatures. This validates the result in Figs. 1 and 2 that increasing temperature from 383 to 423 K (i.e. from B to C) did not much differentiate the outlet CO content.

The corresponding outlet CH_4 content (right *Y*) successively increased with increasing the O/CO ratio, and for each specified O/CO it was larger at the higher temperature of 420 K. While the former will be interpreted in Section 4.1.2, the latter just responded to the enhancement of CH_4 formation with temperature clarified in Figs. 1 and 2. When the outlet CO content reached the desired 10s ppm at the O/CO ratio around 2.3 (v/v), the concentration of the formed CH_4 was correspondingly 200 and 700 ppm or so at 394 and

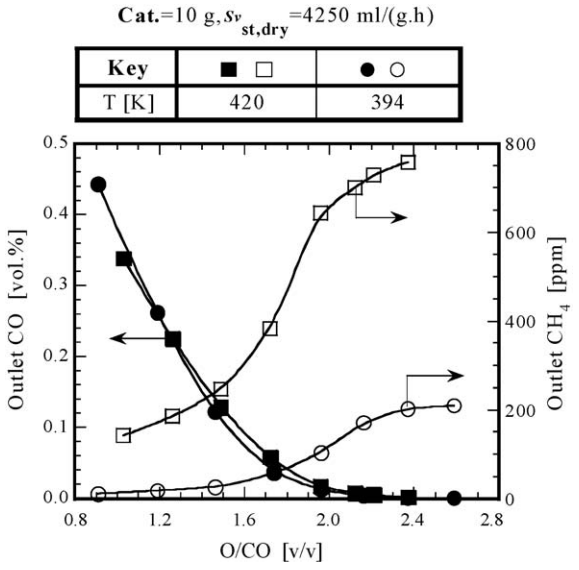

Fig. 3. Necessary O/CO ratio for oxidizing supplied CO down to 10s ppm at the suitable reaction temperatures for CO removal. Feed gas without O_2 (vol.%): 69.8 H_2 + 29.2 CO_2 + 1.00 CO.

420 K, respectively. These CH_4 fractions are obviously much smaller than the removed CO of 1.0%, implicating a limited effect of methanation on the conventionally defined oxidation selectivity S_x and H_2 loss H_{sx}, as will be further analyzed in the succeeding Section 4. Nonetheless, the absolute amount of the methanated CO (>200 ppm) is significant when compared to 10s ppm of the desired outlet CO level. In this sense, the simultaneous methanation is surely critical to catalyst's PROX performance, and in Section 4.1.1 we will show more support for this statement.

Fig. 4 shows the outlet CO (a) and CH_4 (b) fractions measured at different space velocities and initial CO concentrations. The plot of Fig. 4a indicates that at a given O/CO ratio the outlet CO content was higher for the gas with a higher initial CO concentration, although the difference tended to be gradually smaller with increasing the O/CO ratio. This caused eventually a higher O/CO ratio to be required for removing a higher inlet CO content down to the same outlet level, such as 40 ppm (see inset plot, ● versus + or ◯ versus □). On porous-C-supported Ru and Pt catalysts, Snytnikov et al. [31] also reported a higher O/CO ratio required for a gas with a higher inlet CO concentration in order to oxidize the CO down to 10 ppm.

When the gases had the same inlet CO concentration, the outlet CO fraction at a given O/CO ratio appeared little dependent on the space velocity $S_{v(st,dry)}$ until the O/CO was raised to 1.6 (v/v) to let the outlet CO lower than 1000 ppm (Fig. 4a). The further CO removal, however, was closely dependent on $S_{v(st,dry)}$, as one can see from the inset plot of Fig. 4a. That is, a higher $S_{v(st,dry)}$ required a larger O/CO ratio to oxidize the fed CO down to 10s ppm (■ versus □ or ● versus ◯). At $S_{v(st,dry)} = 8500\ ml\ g^{-1}\ h^{-1}$, we even found that it was difficult to remove the supplied CO of 0.99 vol.% (□) to 10 ppm. Consequently, a PROX reactor has to be operated at some

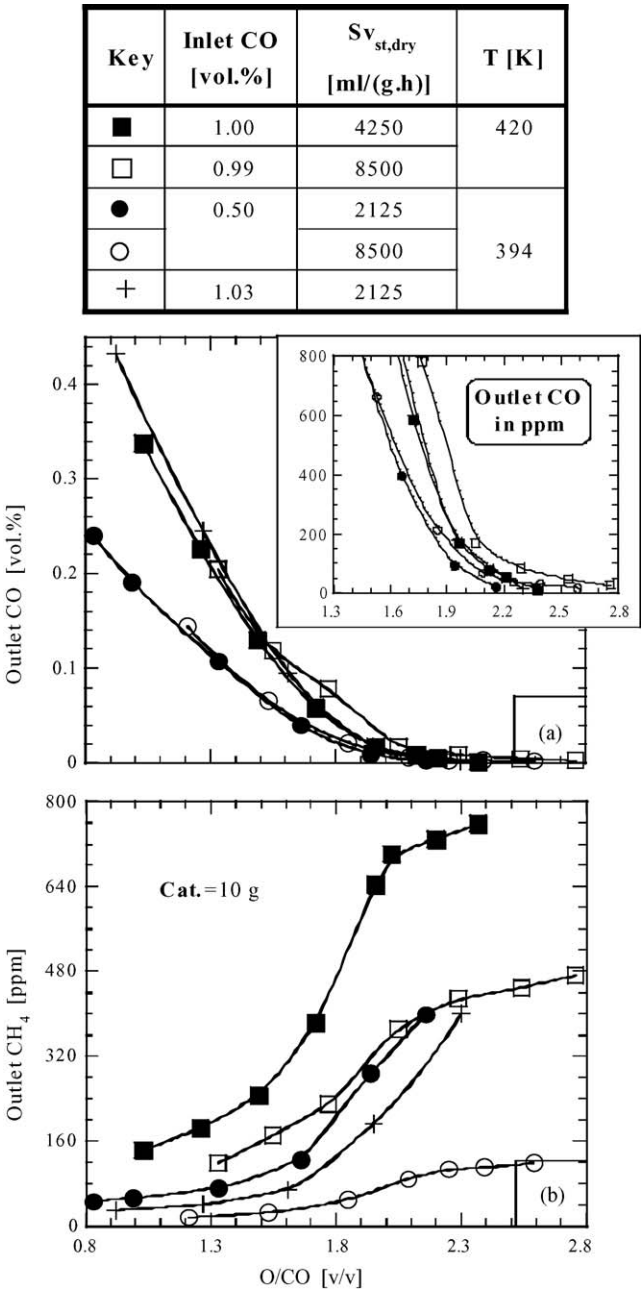

Fig. 4. (a and b) Influences of space velocity and inlet CO concentration on the necessary O/CO ratio for oxidizing CO down to 10s ppm. Feed gas: H_2/CO_2 = 70/30 (v/v) in addition to CO and O_2.

appropriately low space velocities, as was similarly implicated in a few sets of patented data [28,30].

The CH_4 formation corresponding to the CO removal in Fig. 4a is displayed in Fig. 4b. As in Fig. 3, the formed CH_4 increased with raising O/CO ratio in all the tested cases. At any given $S_{v(st,dry)}$ the formed CH_4 was less when the inlet CO concentration was higher (◯ versus □ or + versus ●). A higher initial CO content would cause more adsorbed/dissociated active CO species, i.e. M–CO, in the catalyst bed to lead to quicker CH_4 formation. The actual result is contrary to the anticipation, indicating that the

amount of M–CO does not control the CO methanation reaction under the tested temperatures (<430 K at least). The following reaction,

$$M + CO \rightarrow M\text{–}CO \overset{M\text{–}H/H_2}{\longrightarrow} M\text{–}C \overset{+M\text{–}H}{\longrightarrow} M\text{–}CH \overset{+M\text{–}H}{\longrightarrow} \cdots \overset{+M\text{–}H}{\longrightarrow} CH_4, \quad (10)$$

highlights the elementary chemical steps involved in CO methanation [34,35,39], where M–H refers to the active H species formed via H_2 adsorption/dissociation. Hence, the occurrence of CO methanation is subject not only to the M–CO concentration but also to the available M–H concentration. A higher initial CO concentration causes surely a higher CO-coverage on the catalytic sites, preventing consequently the H_2 adsorption and dissociation and thus suppressing the CH_4 formation. We therefore see that the observed slower CH_4 formation at the higher inlet CO concentration in Fig. 4b was likely due to the H_2 activation, i.e. the formation of M–H that was limited by the corresponding higher CO-coverage.

Once the inlet CO content was given, Fig. 4b shows that the CH_4 formation was faster at lower $S_{v(st,dry)}$ (■ versus □ or ● versus ◯). The lower $S_{v(st,dry)}$ allows a longer reaction time, which would not only enhance CO oxidation to let a smaller O/CO ratio for oxidizing a given amount of CO to the same outlet level but also facilitate the CO and CO_2 methanations to lead to a rapider CH_4 release. Hence, there should be an optimal $S_{v(st,dry)}$ trading these two opposite effects off. Regarding this an analysis in terms of H_2 loss will be delivered in Section 4.2.

In summary, Figs. 3 and 4 demonstrate that the tested industrial 0.5% Ru/Al_2O_3 catalyst is better to be used at space velocities ($S_{v(st,dry)}$) of about 5000 ml g^{-1} h^{-1}. Then, the required O/CO ratio for oxidizing the inlet CO of up to 1.0 vol.% to 10 s ppm should be between 2.5 and 3.0 (v/v). These conditions allow the catalyst to provide a better CO removal performance than most literature-reported Ru catalysts [13,25,28–33]. Over a particularly fabricated Ru/Al_2O_3 catalyst, Wörner et al. [32] acquired a similar performance to oxidize CO to less than 30 ppm at O/CO = 3.0 (v/v) and a space velocity of 5000 h^{-1} between 373 and 433 K. Their tested gas, however, had CO only of 0.42 vol.% (dry-base). Thus, rather higher O/CO ratios (>3.0, v/v) must be required when a gas with more CO (up to 1.0 vol.%) was adopted. Igarashi et al. [21] reported a stoichiometric oxidation of CO at 473 K over a Ru catalyst supported on a material called "mordenite". This is a better performance, but the catalyst, at the present, is surely impossible to be cheaply available. Also on a self-prepared laboratory catalyst (1.0% Ru/C), Snytnikov et al. [31] achieved an oxidation of CO to 10 ppm from 0.5 vol.% at O/CO ratios of about 2.0 (v/v), but its viable temperatures were only within 10 K around 383 K. The CO removal performance shown here is also comparable to the better ones of the available Pt-Ru alloy catalysts [13,14,28,29], while it is better, especially with a wider temperature window, than those of commonly used Pt/Al_2O_3 [18–20,24,33]. Therefore, the presently available commercial Ru catalysts seem to be reliable for use in practical PROX reactors.

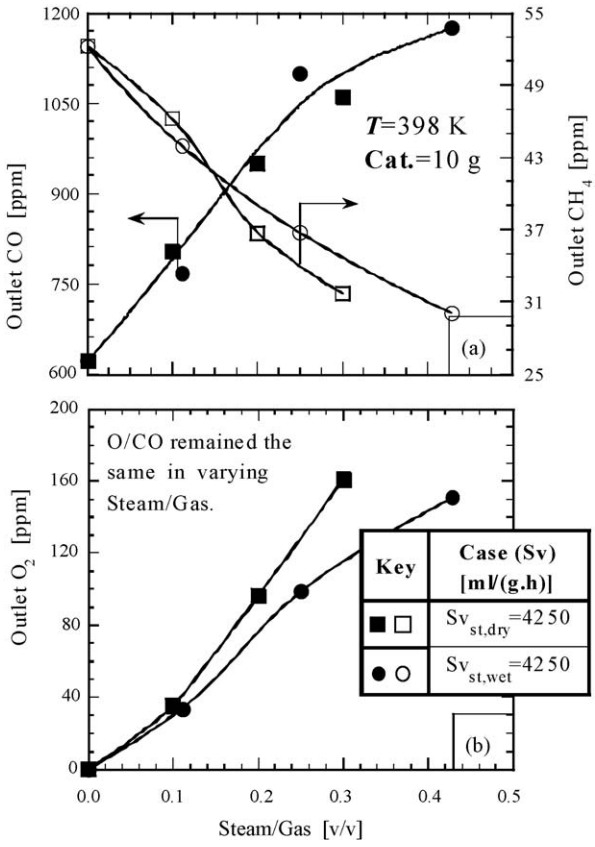

Fig. 5. (a and b) Influence of steam on the catalyst's performance. Dry-base feed gas was 68.9 H_2 + 29.3 CO_2 + 0.80 O_2 + 1.00 CO (vol.%) and the dry gas volume was varied with steam amount for the case with a constant wet-base space velocity $S_{v(st,wet)}$.

3.3. Gas composition influences

Fig. 5 shows the influence of steam on the performance of the tested catalyst at 398 K. The measurement was performed under the same space velocity of either dry-base (■ and □) or wet-base (● and ◯). While the latter ensured an identical real space velocity for the measurements under various steam-to-gas (steam/gas) volumetric ratios (up to 0.45, v/v), the former catered to the case of practical operations and controls based on $S_{v(st,dry)}$. The outlet CO content (■ and ●, left Y in Fig. 5a) increased with raising the steam/gas ratio but exhibited little difference between the two examined cases under the tested conditions. Against this, the released CH_4 amount gradually decreased with raising the steam ratio (□ and ◯, right Y in Fig. 5a) and for a given steam/gas ratio the decrease appeared slightly larger in the case of equi-$S_{v(st,dry)}$. The addition of steam induced an O_2 evolution as well (Fig. 5b), which was promoted with increasing the steam amount and was more significant in the test under the same $S_{v(st,dry)}$ (■).

Hence, the presence of steam in hydrogenous gas definitely reduced the CO removal activity of the catalyst (via both oxidation and methanation). This is a demonstration similar to the observation over zeolite-supported Pt [17] and C-supported Pt and Ru [31] but contrary to that on Pt/Al_2O_3 [20]. On the other hand, Han et al. [26,27] had found that the addition of up to 15 vol.% steam into their simulated reformates little affected the rate and selectivity of CO oxidation on the catalysts 5% Ru/Al_2O_3, 0.5% Pt/Al_2O_3 and 0.5% Rh/MgO. Their adopted high space velocities, say, 36,000–160,000 ml g^{-1} h^{-1}, might be the cause for their different result. Here, at much lower space velocities (for commercial catalyst) we see that the presence of steam likely blocks the adsorption and dissociation of all reactant gases, especially the weakly adsorbed O_2 and H_2, whereby inhibiting, although slightly, the CO oxidation as well as CO methanation. If this is the case, the steam's influence thus has to increase with increasing the steam/gas ratio, as was experimentally shown in Fig. 5. Then, the more promoted O_2 evolution and more suppressed CH_4 formation in the figure for the case of equi-$S_{v(st,dry)}$ should be due to its more steam fed to the catalyst bed under a specified steam/gas ratio.

Fig. 6 examines the steam influence in a wider temperature range of 373–503 K. The measurement method was similar to that for Figs. 1 and 2, and three gases with the steam/gas ratios of 0.0, 0.21 and 0.45 (v/v), respectively, were tested. The resulting data proved first Figs. 1–4 because the inlet CO of 1.0 vol.% was oxidized to 10s ppm from 385 K under O/CO of 2.45 (v/v) (◯, no steam). In this case, the effluent CO was kept at 10s ppm until 503 K, although with a considerable CH_4 release since 433 K (Fig. 6b). Addition of steam (●, steam/gas = 0.21, v/v) delayed the stated CO removal, which makes the outlet CO content less than 100 ppm only at temperatures beyond 410 K (25 K higher than for the steam-free gas). The corresponding CH_4 formation was observed later as well, as can be seen from comparing the data for keys (●) and (◯) in Fig. 6b. At temperatures above 433 K the steam's influence is visible only on the formed CH_4, probably because that the employed high O/CO ratios (>2.4, v/v) firmly kept the outlet CO level of 10s ppm in all the tested cases under such high temperatures (see inset plot in Fig. 6a). Nonetheless, the presence of steam surely narrowed the suitable temperature range of the catalyst for CO removal, as it, when compared to the case of steam-free gas, caused the range to begin from a higher temperature (● versus ◯, inset plot in Fig. 6a). Lifting the O/CO ratio can alleviate the time delay. The data for (◊) and (●) in Fig. 6a indicate that the former case had a higher steam/gas ratio (0.45, v/v) but a shorter delay to reach 10s ppm of the outlet CO levels (from 403 K), showing obviously an improved delay due to its higher O/CO ratio (3.21, v/v). Notwithstanding, the outlet CH_4 content in this case was still lower than that for the cases shown with (●) and (◯) at temperatures above 423 K. This verifies further the steam's suppression effect on methanation clarified in Fig. 5. Similar to Figs. 3 and 4, Fig. 6b (inset plot) proves also the oxygen-facilitated CH_4 formation because the outlet CH_4

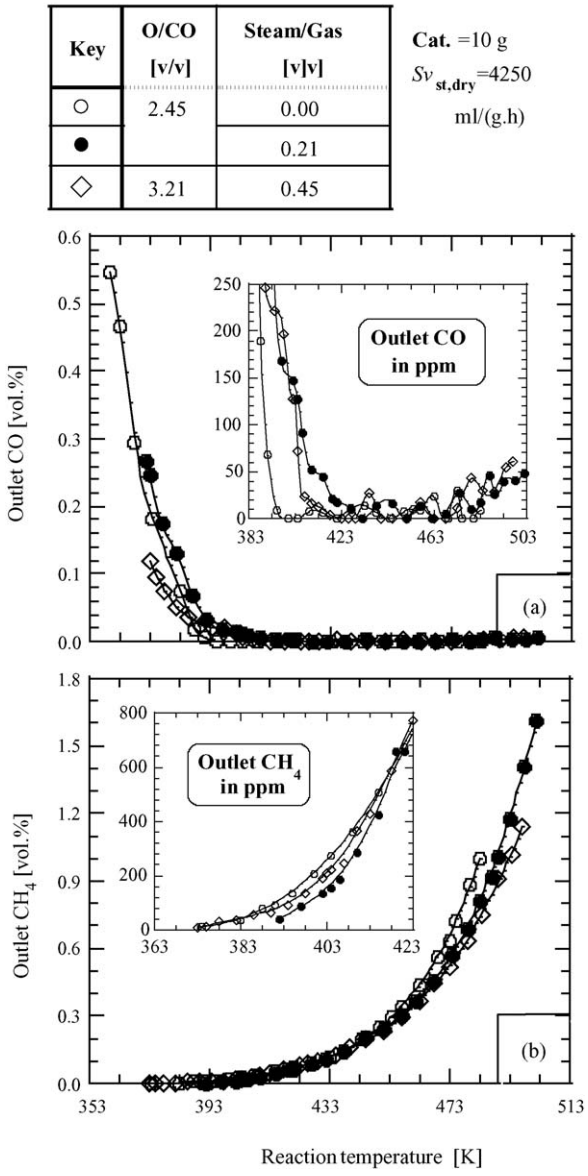

Fig. 6. (a and b) Lowering the inlet CO to 10s ppm at steam-to-gas ratios of up to 0.45 (v/v) and demonstrating the steam influence at different temperatures. Dry feed: CO = 1.00 vol.% and H_2/CO_2 = 70/30 (v/v).

concentration is higher for (◊) than for (●) until 423 K. The steam-hindered O_2 dissociation clarified in Fig. 6b caused the O_2 depletion corresponding to the cases (◯), (●) and (◊) to occur, respectively, at 393, 405 and 415 K.

Fig. 7 shows the influence of CO_2 or equivalently H_2 concentration on the performance of the catalyst at two typical temperatures (383 and 420 K). With increasing the CO_2 fraction from 20 to 34 vol.%, or equivalently decreasing the H_2 concentration from 78 to 64 vol.%, the outlet CO (left *Y*) and CH_4 (right *Y*) contents both tended to decrease slightly. At the higher temperature, the decreasing tendency was more evident, but the decrement was still less than 100 ppm for CO and limited to 20 ppm for CH_4. Hence, for the usually encountered reformates (CO_2: 20–40 vol.%, H_2: 60–80 vol.%), their

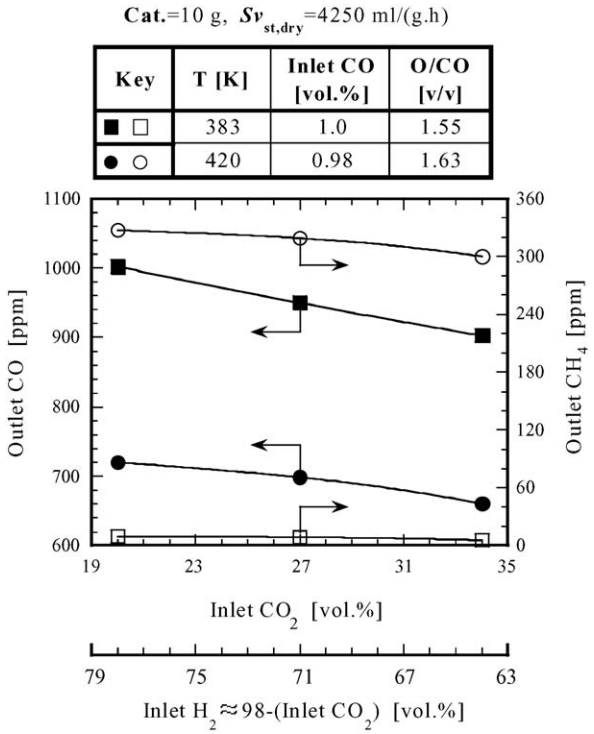

Fig. 7. Influence of CO_2 or H_2 concentration on the catalyst's performance. The H_2 and CO_2 concentrations refer to the values in the gas containing O_2, and they were compensatively varied in the test.

differences in H_2 and CO_2 concentrations would not much affect the performance of Ru catalysts for CO removal and CH_4 formation. Notwithstanding, Fig. 7 reveals a tendency, as anticipated, that a lower H_2 content, which reduces H_2 dissociation, is beneficial to CO removal.

4. Further evaluation

4.1. Selectivity to reactions with CO

4.1.1. Basic features with temperature

This section is devoted to understanding the diagrams of selectivity S_a and S_x shown in Figs. 1 and 2 by considering the competitions not only in reactant adsorption/dissociation but also in the subsequent reactions among dissociated active species. Raising reaction temperature surely enhances H_2 dissociation, while it causes also more O_2 to be dissociated until the supplied O_2 is depleted around point B. Before B, there is no CO methanation through reaction (3), the selectivities S_a and S_x thus must be identical and are subject to the competition of both the H_2 and O_2 dissociations, leading to

$$S_a = S_x = \frac{2 \times \text{dissociated O}_2 - \alpha \times \text{dissociated H}_2}{2 \times \text{dissociated O}_2} = 1 - \frac{\alpha \times \text{dissociated H}_2}{2 \times \text{dissociated O}_2}. \quad (11)$$

where "dissociated O_2" and "dissociated H_2" refer to the moles of activated O_2 and H_2, respectively, and α (<1.0) denotes the proportion of the reacted active H (i.e. M–H) with active O (M–O) via the reaction

$$\text{M–H} + \text{M–O} \rightarrow \text{M–OH} \xrightarrow{+\text{M–H}} \text{H}_2\text{O (g)} \quad (12)$$

in the totally consumed (or dissociated) H_2. Hence, either a faster increase in the "dissociated O_2" than in the "dissociated H_2", which decreases the ratio of "dissociated H_2" over "dissociated O_2", or a decrease in the proportion α with raising temperature can be responsible for the gradual increase in the selectivity until point B clarified in Figs. 1c and 2b. The concern sounds plausible because O_2 has a greater stick coefficient than H_2 [40], which allows the superior adsorption and dissociation of O_2 over that of H_2 to cause the ratio of "dissociated H_2" to "dissociated O_2" to decrease with raising temperature. Meanwhile, the CO oxidation

$$\text{M–CO} + \text{M–O} \rightarrow \text{CO}_2 \quad (13)$$

may be just around its ignition at the low temperatures before point B (<380 K). This allows its kinetic rate to quickly increase with raising temperature to enhance the reaction superiority of M–O with M–CO (Eq. (13)), the dominant species on the catalyst surface, and in turn to reduce the numbers of M–O reacting with M–H (Eq. (12)) to lower the proportion α. The discussed gradual increase in selectivity with raising temperature of up to about 383 K was identified also in Han et al. [26,27] for a 5% Ru/Al_2O_3 catalyst. In our case we further noted that this selectivity increase likely depends on the O/CO ratio and gas' initial CO content (Figs. 1 and 2). Consequently, further studies are worthwhile so as to clarify the prevalent conditions of the phenomenon.

After B, the available "dissociated O_2" amount in the reactor is definite due to the complete dissociation of the supplied O_2. This renders the CO oxidation (Eq. (13)) fully adjusted by the competitive H_2 oxidation (Eq. (12)) or by the coexisting "dissociated H_2" or M–H amount on account of the fact that the kinetic rate of Eq. (12) is much higher than that of Eq. (13) [11,41]. Meanwhile, the methanation of CO (Eq. (3)) starts to cause the conventionally defined selectivity S_x (Eq. (6)) considering CO oxidation only to be logically unsuitable to the analysis of the catalyst's CO removal performance. The overall selectivity S_a (Eq. (7)) taking account of both CO oxidation and methanation thus has to be adopted. In terms of active species S_a can be formulated with

$$S_a = \frac{2 \times \text{supplied O}_2 - \alpha \times \text{dissociated H}_2 + \text{methanated CO}}{2 \times \text{supplied O}_2 + \text{formed CH}_4}, \quad (14)$$

where the term "$2 \times$ supplied $O_2 - \alpha \times$ dissociated H_2" refers actually to the removed CO via CO oxidation. Until point C, the amounts of "Formed CH_4" and "Methanated CO" are almost the same and both are much smaller than "$2 \times$ supplied O_2". Consequently, the selectivity S_a should certainly remain in a constant (e.g., in Fig. 1), given that

the increment in "methanated CO" just compensates for the decrease in oxidized CO resulting from increases in "dissociated H_2". Otherwise, S_a would decrease with increasing temperature when the "methanated CO" is too slow to compensate for the decrease in oxidized CO. The latter occurred in Fig. 2 where the initially higher CO concentration in the feed (1.0 vol.% against 0.5 vol.% in Fig. 1) caused its higher outlet CO content between B and C and in turn its suppressed CH_4 formation.

From C, the "formed CH_4" amount quickly increased with temperature due to the start of CO_2 methanation. This would decrease the selectivity S_a, but the real decrease, according to Eq. (14), should not begin until

$$\frac{\text{Methanated CO}}{\text{Formed CH}_4} < \frac{2 \times \text{supplied O}_2 - \alpha \times \text{dissociated H}_2}{2 \times \text{supplied O}_2} \quad (15)$$

is satisfied. That is, the apparent decrease of S_a with temperature occurs only when the selectivity of methanation toward CO (the left of (15)) becomes smaller than the true oxidation selectivity toward CO defined in the right side of relation (15). Between C and D, it is thus a transition for approaching the conditions satisfying relation (15), consequently allowing S_a to be little varied. After D, the methanation of CO_2 becomes the dominant resource for "formed CH_4", making relation (15) satisfied and accordingly S_a rapidly decreased.

The above analyses implicate that it was the preferential methanation of CO that prevented the CO removal and the overall selectivity S_a from apparently decreasing in the temperature region from B to C, even to D, in Figs. 1c and 2b. On the other hand, Section 4.2 will show that the simultaneous CO and CO_2 methanations only slightly increase the H_2 loss at the suitable working temperatures clarified in Section 3.1. Therefore, we insist that a PROX catalyst be better to have a high methanation activity, in addition to its oxidation activity, for this enables the catalyst to maintain the desired CO removal in a much wider operating temperature window.

4.1.2. Dependences on other parameters

Fig. 8 shows further the variations of selectivity S_a with space velocity, O/CO ratio and gas' initial CO concentration under the above-determined suitable working temperatures. Most of the plotted selectivity values were calculated from the performance data shown in Figs. 3 and 4. The acquired data tend to collapse into a single variation diagram of S_a versus O/CO, except for a detectable split due to different initial CO concentrations at O/CO ratios below 1.8 (v/v). When the initial CO concentration, either 0.5 or 1.0 vol.% in Fig. 8, is given, the result becomes true in the entire range of the tested O/CO ratios. The outlet CO and CH_4 concentrations shown in Figs. 3 and 4 are the cause for the result. There, the outlet CO content shared little difference among the tested inlet CO concentrations (Fig. 4a), reaction temperatures (Figs. 3 and 4a) and space velocities (Fig. 4a) when the O/CO ratio was above 1.8 (v/v). Though the outlet CH_4 concentrations in Figs. 3 (Right *Y*) and 4b appeared evidently different under different temperatures and inlet CO concentrations, their values were limited to 1000 ppm at temperatures below 423 K. With all of these we are thus not surprising that the space velocity, temperature and initial CO concentration had very obscure effect on S_a at O/CO above 1.8 (v/v).

Correspondingly, the higher selectivity for higher inlet CO, which becomes obvious with lowering the O/CO ratio, in the range of O/CO < 1.8 (v/v) would be due to the different outlet CO contents under different inlet CO concentrations. Surely, Fig. 4a shows that a higher inlet CO concentration caused an obviously higher outlet CO content until the O/CO ratio approached 1.8 (v/v). Hence, inside the reactor there must be a higher CO-coverage on the catalyst surface for the gas having a higher initial CO concentration, which certainly limits the H_2 adsorption/dissociation to prevent the H_2 oxidation (also the CO/CO_2 methanation) and to lead to the higher selectivity S_a. With decreasing the O/CO ratio, the difference in the outlet CO content increased between a pair of different inlet CO concentrations (Fig. 4a, 0.5 vol.% versus 1.0 vol.%). This should be just responsible for the gradually larger split of S_a with lower O/CO between the inlet CO concentrations of 0.5 and 1.0 vol.% shown in Fig. 8.

Key	Inlet CO [vol.%]	$Sv_{st,dry}$ [ml/(g.h)]	T [K]	Data source
●	0.50	2125	394	Fig. 4
▼		4250		-
■		8500		Fig. 4
○	1.03	2125	394	Fig. 4
□	1.00	4250		Fig. 3
×	1.00	4250	420	Fig. 4
+	0.99	8500		

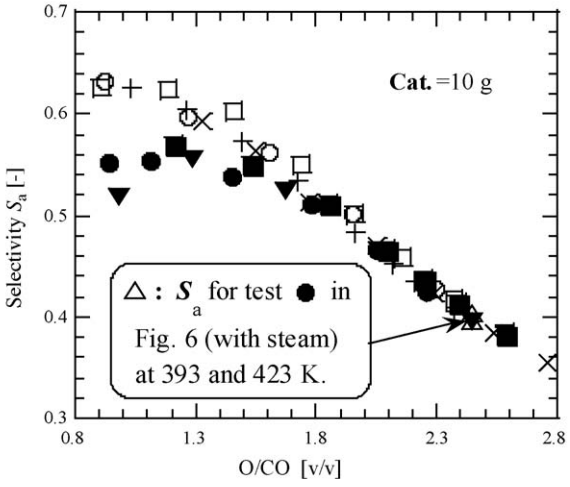

Fig. 8. Selectivity to reactions with CO under different space velocities, CO inlet concentrations and O/CO ratios. More detailed feed and outlet gas compositions are in the figures of "data source".

The selectivity S_a first slightly varied in the range of O/CO < 1.3 (v/v) and then evidently decreased with increasing the O/CO ratio. These again resulted from the corresponding variations of outlet CO concentrations shown in Figs. 3 (Left *Y*) and 4a, where the concentrations first linearly decreased with raising the O/CO ratio until O/CO reached about 1.3 (v/v) and then exhibited a gradually slower decrease. The result demonstrates essentially that the proportion of consumed O_2 in H_2 oxidation is first a constant and then tends to be higher with higher O/CO ratio once the ratio is over, for example, 1.3 (v/v). The assurance of a stable or saturated CO-coverage, which differs the way of enhancing the H_2 dissociation with increasing the O_2 supply, can be considered to be the cause. When the saturated CO coverage is ensured at O/CO, say, <1.3 (v/v), the H_2 dissociation is enhanced with O_2 supply only via the facilitated frequencies at which both O_2 and H_2 attack the originally CO-occupied catalytic sites. Thus, any enhancement in H_2 dissociation and oxidation must be compensated for with a corresponding inhabitation to CO oxidation so that S_a remains to be little varied. On the contrary, if the CO-coverage decreases with raising O/CO (at the other higher O/CO ratios), there must be some CO-uncovered catalytic sites that, while becoming more with higher O_2 supply, work to dissociate and oxidize H_2 without a compensative CO oxidation. With this, the selectivity S_a should have to decrease with raising the O/CO ratio, as is actually shown in Fig. 8 at O/CO over 1.3 (v/v).

Figs. 3 and 4 clarified that a practical PROX reactor has to be operated at the O/CO ratios above 2.3 (v/v). Then, Fig. 8 demonstrates that the corresponding selectivity can be treated as a function of O/CO only and the achievable S_a is possibly up to 0.4 (at O/CO nearby 2.3, v/v). Estimating the S_a for the data shown in Fig. 6 further verified this value. That is, S_a was found to be about 0.4 from 375 to 433 K under the conditions of O/CO = 2.45 (v/v) and steam/gas = 0, while the addition of steam did not much vary this selectivity (see △ in Fig. 8). At the higher O/CO of 3.21 (v/v), S_a was lowered to about 0.3, which is again in consistent with Fig. 8.

4.2. Absolute hydrogen loss

The analysis of absolute H_2 loss H_{sa} (Eq. (8)) as well as H_{sx} (Eq. (9)) is hopeful to gain a better understanding of the PROX performance and its dependences on various influential factors. Fig. 9 correlates H_{sa} and H_{sx} with the O/CO ratio for a few tests. Certainly, raising the O/CO ratio increased the H_2 loss, just as it decreased the selectivity in Fig. 8. Varying the reaction temperature from 373 to 423 K and space velocity from 2250 to 8500 ml g^{-1} h^{-1} did not much change the selectivity S_a in Fig. 8 (at a specified inlet CO content). In Fig. 9, however, a higher temperature (■ versus ●) or lower space velocity (♦ versus ▲) caused surely a larger H_2 loss, although the differences were slight (<0.2 vol.%, see Section 4.1.2 for reasons). Thus, the use of H_2 loss, instead of the selectivity, may allow a better analysis of the parametric dependences of the catalyst's performance.

Key	Inlet CO [vol.%]	T [K]	$Sv_{st,dry}$ [ml/(g.h)]	Data source
■ □	1.00	420	4250	Fig. 3
● ○		394		
◆	0.50	394	2125	Fig. 4
▲ △			8500	

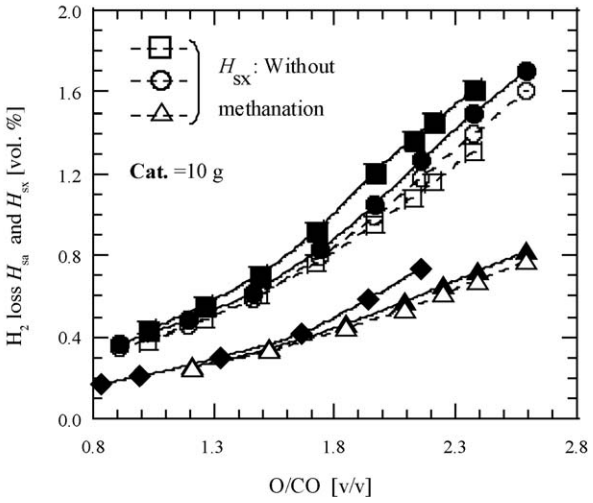

Fig. 9. Absolute hydrogen loss at the suitable reaction temperatures for CO removal and its dependences on the O/CO ratio, space velocity and inlet CO concentration. Detailed feed and outlet gas compositions are in the figures of "data source".

Comparing H_{sa} (solid line) and H_{sx} (dotted line) in Fig. 9 indicates that the calculated H_{sx} is always lower than H_{sa} for a given test, revealing the contribution of methanation to the H_2 loss. We see, however, at the O/CO ratios of about 2.3 (v/v) the methanation-induced H_2 loss was limited to 0.1 vol.% (◯ and △) and 0.4 vol.% (□) for the tests at 394 and 420 K, respectively. These values would be larger at higher O/CO ratios and temperatures, but the H_2 loss due to methanation would be hardly up to 0.5 vol.% under the typical conditions, say, at O/CO < 3.0 (v/v) and temperatures < 430 K, demonstrated in Section 3.1. On the other hand, the largest total (absolute) H_2 loss may reach 2.0 vol.% with an assumed highest inlet CO content of 1.0 vol.% (this agreeing with the selectivity of 0.4 clarified in Fig. 8). Thus, the methanation contribution to the loss is less than 25%, which, compared to the widened temperature window of up to 430 K (even to 445 K), would be surely little important. This shows further that PROX should take advantage of the catalyst's activity for methanating CO, rather than simply treating it as a deadly undesirable side reaction.

Despite the large H_2 loss of up to 2.0 vol.%, the corresponding outlet H_2 concentrations exhibited decreases not much higher than 0.6 vol.% under our tested conditions. Simply, it was because the simultaneous CO methanation as well as the CO and H_2 oxidations decreased the outlet gas vol-

ume. Fig. 9 shows also that the absolute H_2 loss is basically proportional to the initial CO content. This complies with the little differentiated selectivity in Fig. 8 under different inlet CO concentrations, especially at O/CO > 1.5 (v/v). Further, in Fig. 9 H_{sa} is larger at 420 K (■) than at 394 K (●), while H_{sx} (◯ and □) shows the reverse, indicating that the CO methanation at the higher temperature of 420 K made a greater contribution to the CO removal.

Fig. 10 correlates the absolute H_2 loss H_{sa} with the outlet CO concentration. The diagrams are basically grouped on the inlet CO concentration, due to the above-mentioned proportional dependence of H_{sa} on the initial CO content. To reach a specified outlet CO level, the H_2 loss is slightly larger at higher temperatures (■ and □ versus ● and ◯). The space velocity (<8500 ml g^{-1} h^{-1}) appeared little influential to the loss (□ versus ■ or ◇ versus ◆) only when the velocity was low enough to accomplish the desired CO removal. Otherwise, a larger loss may happen to a higher space velocity, as illustrated by the data encircled. Consequently, the suitable space velocity should be decided by examining if it is affordable to the required CO removal rather than by testing its H_2 loss.

Figs. 1 and 2 revealed that it is possible to remove CO down to hundreds of, even to tens of ppm, at O/CO ratios around 1.0 (v/v) by increasing the reaction temperature. Fig. 10 thus compares the H_2 loss in such a case (+, from Fig. 2) with those in the runs under the adaptive working temperatures. Obviously, the H_2 loss is comparable only when the outlet CO concentration is above 0.4 vol.%. At any other lower outlet CO levels the H_2 loss is definitely larger for the test at O/CO = 1.0 (v/v), indicating that for the conventional methanation method it must be extremely difficult, even impossible, to remove CO down to 10s ppm at a reasonable H_2 loss.

Key	Inlet CO [vol.%]	T [k]	$Sv_{st,dry}$ [ml/(g.hr)]	Data source
◆	0.50	394	2125	Fig. 4
◇			8500	
■	1.00	420	4250	
□	0.99		8500	
●	1.03	394	2125	
○	1.00		4250	Fig. 3
+	1.00	varied	4250	Fig. 2

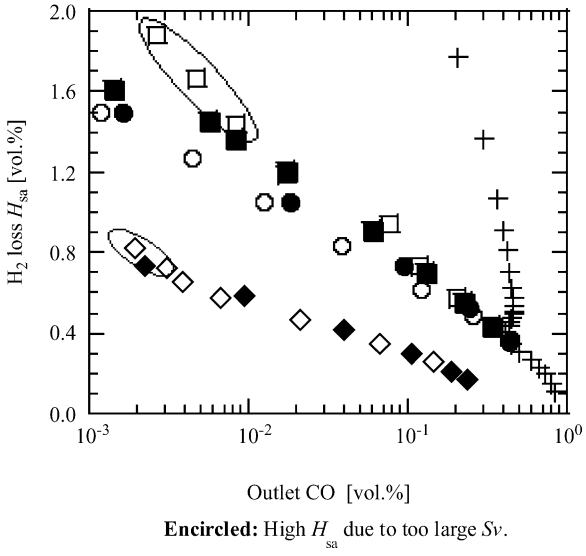

Fig. 10. Absolute hydrogen loss versus outlet CO concentration in different operating cases and test conditions. Detailed conditions, feed and outlet gas compositions are in the figures of "data source".

5. Conclusions

The adaptive reaction temperatures of the tested commercial 0.5% Ru/Al_2O_3 catalyst for removing residual CO from reformates were between 383 and 443 K, preferably between 383 and 423 K. Before 383 K, the oxidized CO rapidly increased with increasing temperature, showing essentially the region controlled by reaction kinetics. Over 443 K, a considerable CO_2 methanation occurred to consume a substantial amount of H_2 and therefore to decrease remarkably the overall selectivity to the CO removal reactions, both CO oxidation and CO methanation. In-between, the decrease in the amount of oxidized CO counteracted the increase in that of methanated CO with raising the reaction temperature to maintain a nearly constant effluent CO content as well as a little varied overall selectivity determined as the ratio of the removed CO amount over the sum of the consumed O_2 and formed CH_4 amounts. The preferential CO adsorption/dissociation on the active catalytic sites assured the CO methanation in prior to CO_2 methanation, but the methanated CO amount appeared subject to the H_2 dissociation or to the available active H amount at the suitable working temperatures for removing CO.

Therefore, the high methanation activity of the tested Ru/Al_2O_3 is likely responsible for its wide working temperature window suitable to CO removal. At these suitable temperatures, the catalyst enabled CO removals down to several tens of ppm at O/CO ratios around 2.5 (v/v) and space velocities of about 5000 h^{-1} from simulated reformates containing steam of up to 0.45 (volume) of dry gas. This CO removal performance corresponded to an overall selectivity of about 0.4. Varying the gas' H_2 content in the range of 60–80 vol.% or CO_2 content in 20–40 vol.% did not much change the CO removal performance of the catalyst, whereas the presence of steam made the working temperatures for the equivalent performance slightly higher (but the shift < 25 K). Further evaluation of the CO removal in terms of the corresponding selectivity and absolute hydrogen loss (i.e. totally reacted H_2) revealed that the O/CO ratio dominated such two evaluation parameters. Space velocity produced a detectable influence on the selectivity and H_2 loss only when it was too

high to afford the desired CO removal or outlet CO level. Of the total hydrogen loss, the contribution of methanation was generally small, which was lower than 25% at the highest suitable working temperature of about 430 K. Compared to the broadened temperature window of 383–443 K of the catalyst for CO removal, this loss was suggested unimportant, making our insistence that the catalyst for PROX be better have a high activity for CO methanation.

Acknowledgements

The authors are grateful to Mr. M. Yamamoto and Ms. N. Imai of AIST Hokkaido for their measuring the catalyst properties and helping the experiments. The final analysis and documentary work for the article were finished during the first author's visit to Germany as an Alexander von Humboldt-Stiftung research fellow.

References

[1] S. Gottesfeld, L. Alamos, N. Mex, US Patent US4,910,099 (1990).
[2] J.J. Baschuk, X. Li, Int. J. Energy Res. 25 (2001) 695–713.
[3] L.P.L. Carrette, K.A. Friedrich, M. Huber, U. Stimming, Phys. Chem. Chem. Phys. 3 (2001) 320–324.
[4] O. Korotkikh, R. Farrauto, Catal. Today 62 (2000) 249–254.
[5] A. Ghenciu, Curr. Opin. Solid State Mater. Sci. 6 (2002) 389–399.
[6] A.N.J. van Keulen, J.G. Reinkingh, US Patent US6,403,049 B1 (2002).
[7] N. Edwards, S.R. Ellis, J.C. Frost, S.E. Golunski, A.N.J. van Keulen, N.G. Lindewald, J.G. Reinkingh, J. Power Sources 71 (1998) 123–128.
[8] K. Ledjeff-Hey, J. Roes, R. Wolters, J. Power Sources 86 (2000) 556–561.
[9] H. Maeda, H. Fukumoto, K. Mitsuda, Electrochemistry 70 (2002) 615–621.
[10] C. Song, Catal. Today 77 (2002) 17–49.
[11] J.M. Zalc, D.G. Löffler, J. Power Sources 111 (2002) 58–64.
[12] D.L. Trimm, Z.I. Önsan, Catal. Rev. 43 (2001) 31–84.
[13] C.D. Dudfield, R. Chen, P.L. Adcock, Int. J. Hydrogen Energy 26 (2001) 763–775.
[14] S.H. Lee, J. Han, K.-Y. Lee, J. Power Sources 109 (2002) 394–402.
[15] M.L. Brown, A.W. Green, Ind. Eng. Chem. 52 (1960) 841–844.
[16] S.H. Oh, R.M. Sinkevitch, J. Catal. 142 (1993) 254–262.
[17] H. Igarashi, H. Uchida, M. Suzuki, Y. Sasaki, M. Watanabe, Appl. Catal. A: Gen. 159 (1997) 159–169.
[18] M.J. Kahlich, H.A. Gasteiger, R.J. Behm, J. Catal. 171 (1997) 93–105.
[19] D.H. Kim, M.S. Lim, Appl. Catal. A: Gen. 224 (2002) 27–38.
[20] A. Manasilp, E. Gulari, Appl. Catal. B: Environ. 37 (2002) 17–25.
[21] H. Igarashi, H. Uchida, M. Watanade, Chem. Lett. (2000) 1262–1263.
[22] P. Bera, A. Gayen, M.S. Hegde, N.P. Lalla, L. Spadaro, F. Frusteri, F. Arena, J. Phys. Chem. B 107 (2003) 6122–6130.
[23] H. Over, M. Muhler, Prog. Surf. Sci. 72 (2003) 3–17.
[24] Y.F. Han, M.J. Kahlich, M. Kinne, R. Behm, J. Phys. Chem. Chem. Phys. 4 (2002) 389–397.
[25] S. Kawatsu, J. Power Sources 71 (1998) 150–155.
[26] Y.-F. Han, M.J. Kahlich, M. Kinne, R. Behm, Appl. Catal. B: Environ. 50 (2004) 209–218.
[27] Y.-F. Han, M. Kinne, R. Behm, Appl. Catal. B: Environ. 52 (2004) 124–134.
[28] A. Satoshi, EU Patent EP 0,955,351 A1 (1999).
[29] A. Satoshi, EU Patent EP 0,743,694 A1 (1996).
[30] S.F. Abdo, C.A. DeBoy, G.F. Schroeder, US Patent US6,299,995 (2001).
[31] P.V. Snytnikov, V.A. Sobyanin, V.D. Belyaev, P.G. Tsyrulnikov, N.B. Shitova, D.A. Shlyapin, Appl. Catal. A: Gen. 239 (2003) 149–156.
[32] A. Wörner, C. Friedrich, R. Tamme, Appl. Catal. A: Gen. 245 (2003) 1–14.
[33] T. Utaka, T. Takeguchi, R. Kikuchi, K. Eguchi, Appl. Catal. A: Gen. 246 (2003) 117–124.
[34] F. Solymosi, A. Erdöhelyi, M. Kocsis, J. Chem. Soc. Faraday Trans. 1 (77) (1981) 1003–1012.
[35] D.P. VanderWiel, M. Pruski, T.S. King, J. Catal. 188 (1999) 186–202.
[36] M. Nawdali, H. Ahlafi, G.M. Pajonk, D. Bianchi, J. Mol. Catal. A: Chem. 162 (2000) 247–256.
[37] Z.-G. Zhang, G. Xu, X. Chen, K. Honda, T. Yoshida, Fuel Process Technol. 85 (2004) 1213–1229.
[38] G. Xu, X. Chen, K. Honda, Z.-G. Zhang, AIChE J. 50 (2004) 2467–2480.
[39] M.A. Henderson, S.D. Worley, J. Phys. Chem. 89 (1985) 1417–1423.
[40] Y. Nishiyama, H. Wise, J. Catal. 32 (1974) 50–62.
[41] V.P. Zhdanov, B. Kasemo, Surf. Sci. Rep. 20 (1994) 111–189.